Nanoscale Research Letters
a SpringerOpen Journal

NANO EXPRESS   **Open Access**

Structural and nanomechanical properties of BiFeO₃ thin films deposited by radio frequency magnetron sputtering

Sheng-Rui Jian[1*], Huang-Wei Chang[2], Yu-Chin Tseng[1], Ping-Han Chen[2] and Jenh-Yih Juang[3]

Abstract

The nanomechanical properties of BiFeO₃ (BFO) thin films are subjected to nanoindentation evaluation. BFO thin films are grown on the Pt/Ti/SiO₂/Si substrates by using radio frequency magnetron sputtering with various deposition temperatures. The structure was analyzed by X-ray diffraction, and the results confirmed the presence of BFO phases. Atomic force microscopy revealed that the average film surface roughness increased with increasing of the deposition temperature. A Berkovich nanoindenter operated with the continuous contact stiffness measurement option indicated that the hardness decreases from 10.6 to 6.8 GPa for films deposited at 350°C and 450°C, respectively. In contrast, Young's modulus for the former is 170.8 GPa as compared to a value of 131.4 GPa for the latter. The relationship between the hardness and film grain size appears to follow closely with the Hall–Petch equation.

Keywords: BiFeO₃ thin films, XRD, AFM, Nanoindentation, Hardness

Background

Multiferroic materials exhibit some unique characteristics with the co-existence of at least two kinds of long-range ordering among ferroelectricity (or antiferroelectricity), ferromagnetism (or antiferromagnetism), and ferro-elasticity. Single-phase compounds in which both ferro-magnetism and ferroelectricity arise independently and may couple to each other to give rise to magneto-electric interactions are ideal materials for novel functional device applications but are unfortunately rare in nature [1]. BiFeO₃ (BFO) is one of the most important multiferroic materials so far discovered, which has a ferroelectric Curie temperature of 1,103 K [2,3] and an antiferromagnetic Néel temperature of 643 K [4]. In addition to its interesting optical properties [5], strong coupling between ferro-electric and magnetic orders is observed in BFO at room temperature, making it a strong candidate for realizing room-temperature multiferroic devices [6,7]. However, while most of the researches have been concentrated on the abovementioned magneto-electric characteristics of

BFO, researches on the mechanical characteristics of this prominent functional material have been largely ignored. In particular, since the mechanical properties of materials are size-dependent, the properties obtained from thin films may substantially deviate from those of the bulk material. In view of the fact that most practical applications of functional devices are fabricated with thin films, it is desirable to carry out precise measurements of the mechanical properties of BFO thin films.

Because of its high sensitivity, excellent resolution, and easy operation, nanoindentation has been widely used for characterizing the mechanical properties of various nanoscale materials [8,9] and thin films [10-12]. Among the mechanical characteristics of interest, the hardness, Young's modulus, and the elastic/plastic deformation behaviors of the interested material can be readily obtained from nanoindentation measurements. For instance, by analyzing the load–displacement curves obtained during the nanoindentation following the methods proposed by Oliver and Pharr [13], the hardness and Young's modulus of the test material can be easily obtained. In general, in order to avoid the complications arising from the substrate material, the contact depths of the indenter need to be less than 10% of the film thickness to obtain

* Correspondence: srjian@isu.edu.tw
[1]Department of Materials Science and Engineering, I-Shou University, Kaohsiung 840, Taiwan
Full list of author information is available at the end of the article

intrinsic film properties [14]. On the other hand, it is very difficult to obtain meaningful analytical results for indentation depths less than 10 nm because of the equipment limitations. Hence, for films thinner than 100 nm, it is almost impossible to obtain results without being influenced by responses from the substrate. In order to gain some insights on the substrate influences and obtain the intrinsic properties for films thinner than 100 nm, it is essential to monitor the mechanical properties as a function of depth. Herein, in this study, a continuous stiffness measurement (CSM) mode [15] was adopted to continuously monitor the hardness and Young's modulus values of BFO films as a function of the indentation depth. Variations in mechanical properties for BFO thin films deposited under different conditions are discussed in conjunction with the crystalline structure, grain size, and surface morphology of the resultant films.

Methods

The BFO thin films investigated in this study were deposited on Pt/Ti/SiO$_2$/Si(100) substrates at the deposition temperatures of 350°C, 400°C, and 450°C, respectively. The deposition process was conducted in a radio frequency magnetron sputtering system, and a commercially available Bi$_{1.1}$FeO$_3$ pellet was used as the target. The base pressure of the sputtering chamber was better than 1×10^{-7} Torr. During deposition, a mixed gas of Ar/O$_2$ = 4:1 with a total pressure was introduced, and the input power was maintained at 80 W. All of the BFO thin films are about 200 nm thick. The composition of the film was identified by an energy-dispersive X-ray analysis and double checked by X-ray fluorescence analysis. The crystal structure of BFO thin films was analyzed by X-ray diffraction (X'Pert XRD, PANalytical B. V., Almelo, The Netherlands; CuKα, λ = 1.5406 Å). The surface features were examined by atomic force microscopy (AFM; Topometrix-Accures-II, Topometrix Corporation, Santa Clara, CA, USA). The root mean square of the surface roughness, R_{RMS}, was calculated by the following equation [16]:

$$R_{RMS} = \sqrt{\frac{1}{N}\sum_{n=1}^{N} r_n^2} \qquad (1)$$

Here N is the number of data and r_n is the surface height of the nth datum.

Nanoindentation experiments were preformed on a MTS Nano Indenter® XP system (MTS Nano Instruments, Knoxville, TN, USA) with a three-sided pyramidal Berkovich indenter tip by using the CSM technique [15]. This technique is accomplished by imposing a small, sinusoidal varying force on top of the applied linear force that drives the motion of the indenter. The displacement response of the indenter at the excitation frequency and the phase angle between the force and displacement are measured continuously as a function of the penetration depth. Solving for the in-phase and out-of-phase portions of the displacement response gives rise to the determination of the contact stiffness as a continuous function of depth. As such, the mechanical properties changing with respect to the indentation depth can be obtained. The nanoindentation measurements were carried out as follows: First, prior to applying loading on BFO thin films, nanoindentation was conducted on the standard fused silica sample to obtain the reasonable range (Young's modulus of fused silica is 68~72 GPa). Then, a constant strain rate of 0.05 s^{-1} was maintained during the increment of load until the indenter reached a depth of 60 nm into the surface. The load was then held at the maximum value of loading for 10 s in order to avoid the creep which might significantly affect the unloading behavior. The indenter was then withdrawn from the surface at the same rate until the loading has reduced to 10% of the maximum load. Then, the indenter was completely removed from the material. In this study, constant strain rate was chosen in order to avoid the strain-hardening effects. At least 20 indentations were performed on each sample, and the distance between the adjacent indents was kept at least 10 μm apart to avoid interaction.

In nanoindentation tests, the hardness is defined as the applied indentation load divided by the projected contact area as follows:

$$H = \frac{P_{max}}{A_p} \qquad (2)$$

where A_p is the projected contact area between the indenter and the sample surface at the maximum indentation load, P_{max}. For a perfectly sharp Berkovich indenter, the projected area A_p is given by $A_p = 24.56h_c^2$ with h_c being the true contact depth.

The elastic modulus of the sample can be calculated based on the relationships developed by Sneddon [17]: $S = 2\beta E_r \sqrt{A_p}/\sqrt{\pi}$. Here S is the contact stiffness of the material, and β is a geometric constant with β = 1.00 for the Berkovich indenter, respectively. The reduced elastic modulus, E_r, can be calculated from the following equation:

$$\frac{1}{E_r} = \frac{1-\nu_{film}^2}{E_{film}} + \frac{1-\nu_i^2}{E_i} \qquad (3)$$

Here ν is Poisson's ratio, and the subscripts i and f denote the parameters for the indenter and the BFO thin films, respectively. For the diamond indenter tip, E_i = 1,141 GPa and ν_i = 0.07, and ν_{film} = 0.25 is assumed for

BFO thin films in this work. It is generally accepted that the indentation depth should never exceed 30% of the film thickness to avoid the substrate effect on hardness and modulus measurements [18]. Our samples and test methodology were considered as adequate based on this concept. In addition, because of the fact that it enters as $\left(1-\nu_{\text{film}}^2\right)$ in the calculation of E, an error in the estimation of Poisson's ratio does not produce a significant effect on the resulting value of the elastic modulus of thin films [19].

Results and discussion

Figure 1 shows the XRD results of BFO thin films obtained with deposition temperatures of 350°C, 400°C, and 450°C, respectively. It is evident that the intensity and the full width at half maximum (FWHM) of the BFO(110) diffraction peak are both improved with the increasing deposition temperature, indicating a tendency of better film crystallinity and increased grain size. The grain size, D, can be estimated according to Scherrer's equation [20]:

$$D = \frac{0.9\lambda}{B\cos\theta} \tag{4}$$

where λ, B, and θ are the X-ray wavelength, the FWHM of the BFO(110) diffraction peak, and the corresponding Bragg's diffraction angle, respectively. The estimated

Figure 1 XRD patterns of BFO thin films deposited at various deposition temperatures. (**a**) 350°C, (**b**) 400°C, and (**c**) 450°C.
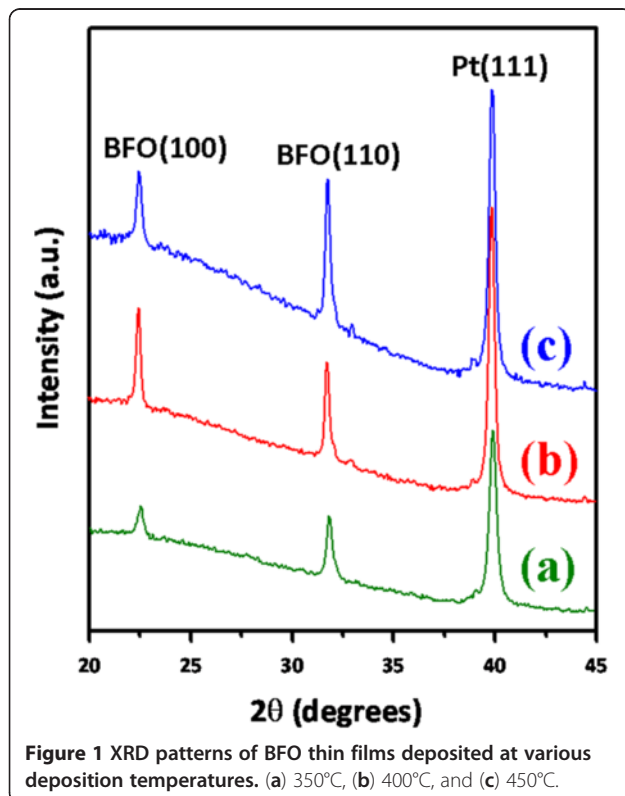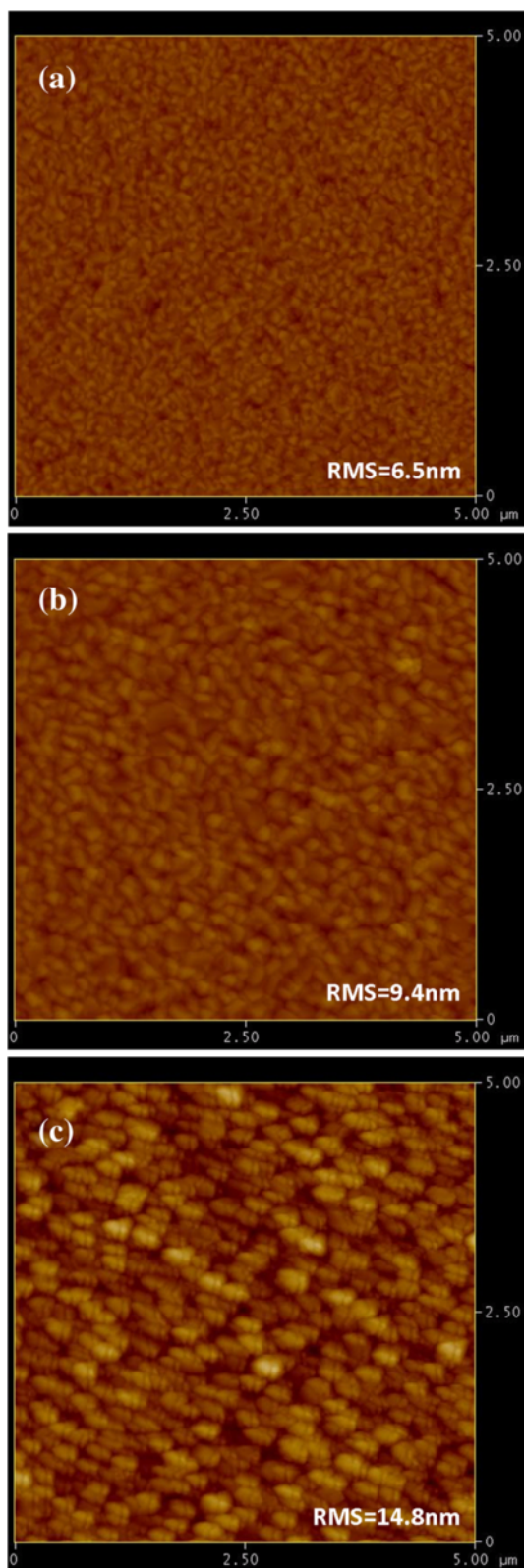
grain sizes for BFO thin films deposited at 350°C, 400°C, and 450°C are 24.5, 30.6, and 51.2 nm, respectively. As can be seen below, consistent results were obtained from the AFM examinations.

As shown in Figure 2, the AFM observations reveal that the R_{RMS} values for BFO thin films deposited at 350°C, 400°C, and 450°C are 6.5, 9.4, and 14.8 nm, respectively. Moreover, as shown in Figure 2a,b,c, the BFO thin films all exhibit similar dense, homogeneous microstructures, albeit that the grain size appears to increase with increasing deposition temperature. The average grain size obtained from image analysis on the AFM images indeed gave consistent results with those obtained from XRD analyses. Namely, the microstructure of BFO films are polycrystalline, and the grain size increases from about 24.5 nm for thin films deposited at 350°C to about 51.2 nm for thin films deposited at 450°C. This is attributed to the additional thermal energy acquired from higher deposition temperature, which may further facilitate the coalescence of the adjacent grains (or nuclei) and result in larger grains during deposition process.

Figure 3a displays the typical load–displacement (*P-h*) curves for the BFO film deposited at 350°C, which reflects the general deformation behavior during the penetration of a Berkovich indenter loaded with the CSM mode. The *P-h* response obtained by nanoindentation contains information about the elastic behavior and plastic deformation and thus can be regarded as the 'fingerprint' of the properties of BFO thin films. The curve appears to be smooth and regular. The absence of any discontinuities along either the loading or unloading segment is in sharp contrast to those observed in GaN thin films [21,22] and in single-crystal Si [23,24], indicating that neither twinning nor pressure-induced phase transformation is involved here.

Figure 3b,c presents the hardness and Young's modulus versus penetration depth curves for the BFO film deposited at 350°C, 400°C, and 450°C, respectively. The curves can be roughly divided into two stages, namely, an initial increase to a maximum value followed by a subsequent decrease to a constant value. The initial sharp increase in hardness at a small penetration depth is usually attributed to the transition from purely elastic to elastic/plastic contact. Only under the condition of a fully developed plastic zone does the mean contact pressure represent the hardness. When there is no plastic zone, or only a partially formed plastic zone, the mean contact pressure measured according to the Oliver and Pharr method [13] is usually smaller than the nominal hardness. After the first stage, the hardness decreases in a rather meandering manner, presumably involving massive dislocation and grain boundary activities relevant to the fine grain structure of the films. Nevertheless, the

Figure 2 AFM images of BFO thin films deposited at various deposition temperatures. (**a**) 350°C, (**b**) 400°C, and (**c**) 450°C, respectively.
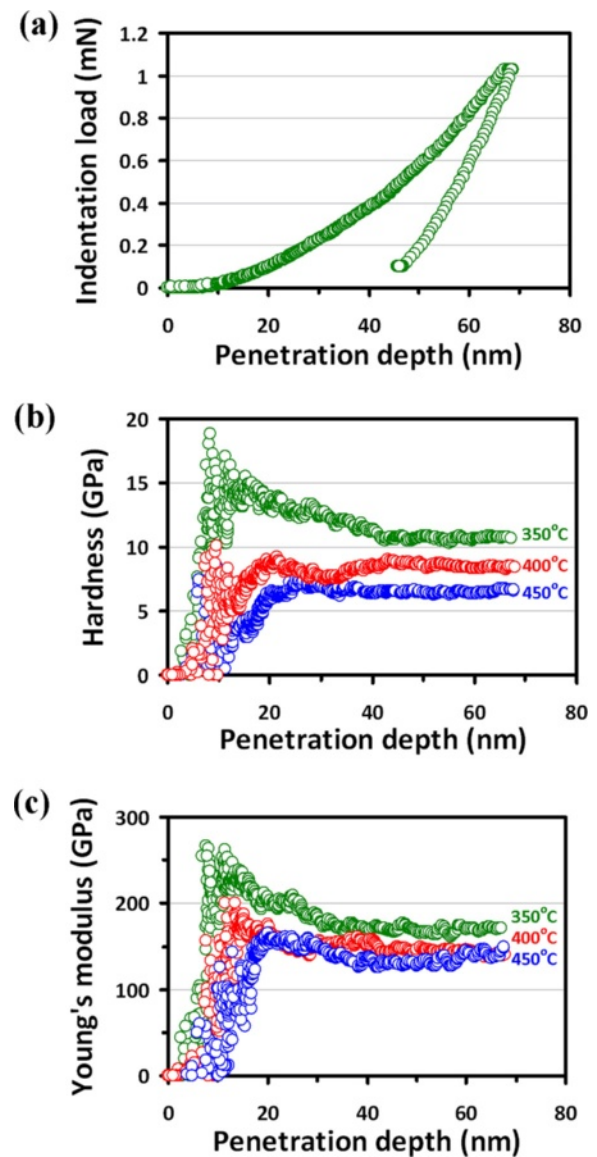
Figure 3 Nanoindentation results. (**a**) A typical load-displacement curve for BFO thin films deposited at 350°C. (**b**) The hardness-displacement curves. (**c**) Young's modulus-displacement curves for BFO thin films deposited at various deposition temperatures.

fact that it eventually reaches a constant value at a moderate indentation depth indicates that a single material is being measured. The hardness values obtained at this stage, thus, can be regarded as the intrinsic properties of the films. The penetration depth dependence of Young's modulus (Figure 3c) behaves similarly as that of the hardness. Consequently, both mechanical parameters were determined using the curves obtained from the CSM loading scheme (Figure 3b,c) by taking the average values within the penetration depth of 40 to 60 nm. This range of penetration depth was chosen intentionally to be deep enough for observing plastic deformation during indentation yet

to be shallow enough to avoid the complications arising from the effects of surface roughness [25] and substrate [18]. Table 1 summarizes the hardness and Young's modulus for various BFO thin films obtained from different deposition methods and indentation operation modes.

It is well known that the dependence of material hardness on the grain size can be described by the phenomenological 'Hall-Petch' equation [27]:

$$H(D) = H_0 + k_{\mathrm{H-P}} D^{-1/2} \qquad (5)$$

where H_0 and $k_{\mathrm{H-P}}$ are denoted as the lattice friction stress and the Hall–Petch constant, respectively. A plot of the hardness versus $D^{-1/2}$ data for BFO thin films deposited at various temperatures is displayed in Figure 4. We note that although the grain size of BFO thin films remains relatively small as compared to that of the usual metallic materials, the data still follow pretty closely to the Hall–Petch relation, and the so-called negative Hall–Petch effect [28] is not observed here. The dashed line represents the fit to the Hall–Petch equation for the experimental data, which gives

$$H(D) = 1.03 + 43.12\, D^{-1/2} \qquad (6)$$

which indicates a probable lattice friction stress of 1.03 GPa, and the Hall–Petch constant of 43.12 GPa nm$^{1/2}$ for BFO thin films also indicates the effectiveness of the grain boundary in hindering the dislocation movements.

Furthermore, it is evident that both the hardness and Young's modulus of BFO thin films decrease monotonically with increasing deposition temperature. The corresponding hardness values (Young's modulus) are 10.6 (170.8), 8.5 (147.6), and 6.8 (131.4) GPa for BFO thin films deposited at 350°C, 400°C, and 450°C, respectively. Since the higher deposition temperature leads to the larger grain size for BFO thin films, as we have discussed previously, it is reasonable to consider that the decrease of hardness and Young's modulus might be mainly due to the grain size effect [29].
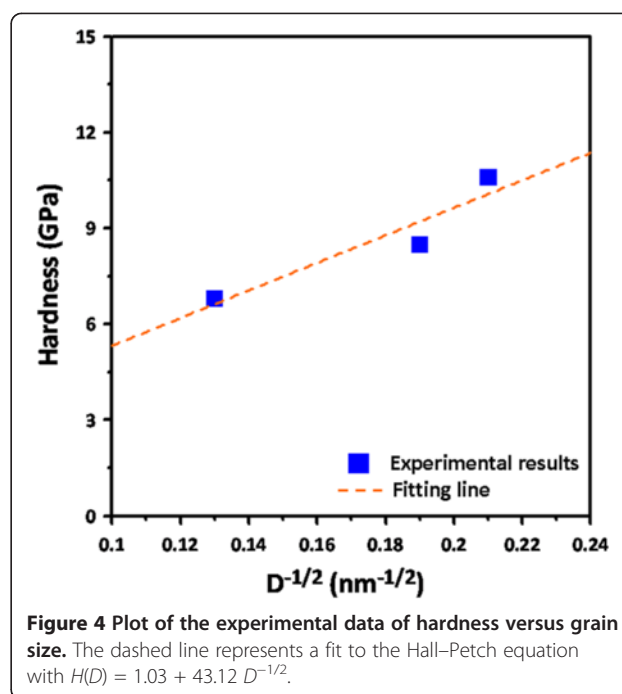
Conclusion

In conclusion, we have carried out the XRD, AFM, and nanoindentation techniques to investigate the fundamental

Figure 4 Plot of the experimental data of hardness versus grain size. The dashed line represents a fit to the Hall–Petch equation with $H(D) = 1.03 + 43.12\ D^{-1/2}$.

nanomechanical properties and their correlations with the microstructural features of the technologically important multiferroic BFO thin films. The XRD analysis showed that BFO thin films were equiaxial polycrystalline in nature, albeit that the predominant (110) orientation and a rougher surface morphology were gradually developed with increasing deposition temperature. Nanoindentation results indicated that, depending on the grain size which is intimately related to the deposition temperature, BFO thin films have hardness ranging from 6.8 to 10.6 GPa and Young's modulus ranging from 131.4 to 170.8 GPa with the higher values corresponding to lower deposition temperatures. In addition, the hardness of BFO thin films appears to follow the Hall–Petch equation rather satisfactorily, and the Hall–Petch constant of 43.12 GPa nm$^{1/2}$ suggests the effectiveness of grain boundary in inhibiting the dislocation movement in BFO thin films.

Authors' information

SRJ is an associate professor and YCT is a designated topic student (in the Department of Materials Science and Engineering, I-Shou University, Kaohsiung, Taiwan). HWC is an associate professor and PHC is a master student (in the Department of Applied Physics, Tunghai University, Taichung, Taiwan). JYJ is a professor (in the Department of Electrophysics, National Chiao Tung University, Hsinchu, Taiwan).

Authors' contributions

SRJ designed the project of experiments; performed the XRD, AFM, and nanoindentation analyses; and drafted the manuscript. YCT dealt with the experimental data. HWC and PHC carried out the growth of BFO thin films, and JYJ participated in the paper discussion. All authors read and approved the final manuscript.

Table 1 Hardness and Young's modulus of BFO thin films obtained from various deposition methods

	H (GPa)	E (GPa)
Radio frequency magnetron sputtering-derived BFO[a]		
350°C	6.8	131.4
400°C	8.5	147.6
450°C	10.6	170.8
Sol–gel-derived BFO [26]	2.8~3.8	26~51

[a]The present work.

Author details

[1]Department of Materials Science and Engineering, I-Shou University, Kaohsiung 840, Taiwan. [2]Department of Applied Physics, Tunghai University, Taichung 407, Taiwan. [3]Department of Electrophysics, National Chiao Tung University, Hsinchu 300, Taiwan.

References

1. Hill NA: **Why are there so few magnetic ferroelectrics?** *J Phys Chem B* 2000, **104**:6694.
2. Neaton JB, Ederer C, Waghmare UV, Spaldin NA, Rabe KM: **First-principles study of spontaneous polarization in multiferroic BiFeO$_3$.** *Phys Rev B* 2005, **71**:014113.
3. Simões AZ, Aguiar EC, Gonzalez AHM, Andrés J, Longo E, Varela JA: **Strain behavior of lanthanum modified BiFeO$_3$ thin films prepared via soft chemical method.** *J Appl Phys* 2008, **104**:104115.
4. Catalan G, Scott JF: **Physics and applications of bismuth ferrite.** *Adv Mater* 2009, **21**:2463.
5. Wei J, Xue D, Xu Y: **Photoabsorption characterization and magnetic property of multiferroic BiFeO3 nanotubes synthesized by a facile sol–gel template process.** *Scripta Mater* 2008, **58**:45.
6. Kim HH, Dho JH, Qi X, Kang SK, Macmanus-Driscoll JL, Kang DJ, Kim KN, Blamire MG: **Growth and characterization of BiFeO3 film for novel device applications.** *Ferroelectrics* 2006, **333**:157.
7. Vasudevan RK, Liu Y, Li J, Liang WI, Kumar A, Jesse S, Chen YC, Chu YH, Nagarajan V, Kalinin SV: **Nanoscale control of phase variants in strain-engineered BiFeO$_3$.** *Nano Lett* 2011, **11**:3346.
8. Ni H, Li XD, Gao H: **Elastic modulus of amorphous SiO$_2$ nanowires.** *Appl Phys Lett* 2006, **88**:043108.
9. Ni H, Li XD, Cheng G, Klie R: **Elastic modulus of single-crystal GaN nanowires.** *J Mater Res* 2006, **21**:2882.
10. Jian SR, Juang JY, Chen NC, Jang JSC, Huang JC, Lai YS: **Nanoindentation-induced structural deformation in GaN/AlN multilayers.** *Nanosci Nanotechnol Lett* 2010, **2**:315.
11. Jian SR, Ku SA, Luo CW, Jang JY: **Nanoindentation of GaSe thin films.** *Nanoscale Res Lett* 2012, **7**:403.
12. Jian SR, Lin YY, Ke WC: **Effects of thermal annealing on the structural, electrical and mechanical properties of Al-doped ZnO thin films deposited by radio-frequency magnetron sputtering.** *Sci Adv Mater* 2013, **5**:7.
13. Oliver WC, Pharr GM: **An improved technique for determining hardness and elastic modulus using load and displacement sensing indentation experiments.** *J Mater Res* 1992, **7**:1564.
14. Tsui TY, Pharr GM: **Substrate effects on nanoindentation mechanical property measurement of soft films on hard substrates.** *J Mater Res* 1999, **14**:292.
15. Li XD, Bhushan B: **A review of nanoindentation continuous stiffness measurement technique and its applications.** *Mater Charact* 2002, **48**:11.
16. Miyoshi K, Chung YW: *Surface Diagnostics in Tribology: Fundamental Principles and Applications.* Singapore: World Scientific Publishing; 1993.
17. Sneddon IN: **The relation between load and penetration in the axisymmetric Boussinesq problem for a punch of arbitrary profile.** *Int J Eng Sci* 1965, **3**:47.
18. Li XD, Gao H, Murphy CJ, Caswell KK: **Nanoindentation of silver nanowires.** *Nano Lett* 2003, **11**:1495.
19. Hu LJ, Zhang XW, Sun Y, Williams RJJ: **Hardness and elastic modulus profiles of hybrid coatings.** *J Sol–gel Sci Tech* 2005, **34**:41.
20. Cullity BD, Stock SR: *Element of X-Ray Diffraction.* New Jersey: Prentice Hall; 2001:170.
21. Jian SR: **Berkovich indentation-induced deformation behaviors of GaN thin films observed using cathodoluminescence and cross-sectional transmission electron microscopy.** *Appl Surf Sci* 2008, **254**:6749.
22. Jian SR, Ke WC, Juang JY: **Mechanical characteristics of Mg-doped GaN thin films by nanoindentation.** *Nanosci Nanotechnol Lett* 2012, **4**:598.
23. Bradby JE, Williams JS, Wong-Leung J, Swain MV, Munroe P: **Transmission electron microscopy observation of deformation microstructure under spherical indentation in silicon.** *Appl Phys Lett* 2000, **77**:3749.
24. Jian SR, Chen GJ, Juang JY: **Nanoindentation-induced phase transformation in (110)-oriented Si single crystals.** *Curr Opin Solid State Mater Sci* 2010, **14**:69.
25. Bobji MS, Biswas SK, Pethica JB: **Effect of roughness on the measurement of nanohardness-a computer simulation study.** *Appl Phys Lett* 1997, **71**:1059.
26. Sen P, Dey A, Mukhopadhyay AK, Bandyopadhyay SK, Himanshu AK: **Nanoindentation behavior of nano BiFeO$_3$.** *Ceram Int* 2012, **38**:1347.
27. Venkatraman R, Bravman JC: **Separation of film thickness and grain-boundary strengthening effects in Al thin-films on Si.** *J Mater Res* 2040, **1992**:7.
28. Conrad H, Narayan J: **On the grain size softening in nanocrystalline materials.** *Scripta Mater* 2000, **42**:1025.
29. Delobelle P, Guillon O, Fribourg-Blanc E, Soyer C, Cattan E, Rèminens D: **True Young modulus of Pb(Zr, Ti)O$_3$ films measured by nanoindentation.** *Appl Phys Lett* 2004, **85**:5185.